May 2007

The Nasal Cavity Is a Route for Prion Infection in Hamsters

Anthony E. Kincaid
Creighton University

Jason C. Bartz
Creighton University, jbartz@creighton.edu

JOURNAL OF VIROLOGY, May 2007, p. 4482–4491 Vol. 81, No. 9
0022-538X/07/$08.00+0 doi:10.1128/JVI.02649-06

The Nasal Cavity Is a Route for Prion Infection in Hamsters▽

Anthony E. Kincaid[1,2]* and Jason C. Bartz[3]

Department of Physical Therapy,[1] Department of Biomedical Sciences,[2] and Department of Medical Microbiology and Immunology,[3] Creighton University, Omaha, Nebraska 68178

Received 30 November 2006/Accepted 9 January 2007

Animals that naturally acquire the prion diseases have a well-developed olfactory sense that they utilize for a variety of basic behaviors. To assess the potential for the nasal cavity to serve as a point of entry for prion diseases, a small amount of prion-infected brain homogenate was placed inferior to the nostrils of hamsters, where it was immediately sniffed into the nasal cavity. Hamsters extranasally inoculated with the HY strain of transmissible mink encephalopathy (TME) agent had an incubation period that was not significantly different from per os inoculation of the same dose of the HY TME agent. However, the efficiency of the nasal route of inoculation was determined to be 10 to 100 times greater based on endpoint dilution analysis. Immunohistochemistry on tissues from hamsters killed at 2-week intervals after inoculation was used to identify the disease-associated form of the prion protein (PrP^d) to determine the route of prion neuroinvasion. Nasal mucosa-associated lymphoid tissue and submandibular lymph nodes initially accumulated PrP^d as early as 4 weeks postinfection. PrP^d was first identified in cervical lymph nodes at 8 weeks, in the mesenteric lymph nodes, spleen, and Peyer's patches at 14 weeks, and in the tongue 20 weeks after inoculation. Surprisingly, there was no evidence of PrP^d in olfactory epithelium or olfactory nerve fascicles at any time after inoculation. Therefore, the HY TME agent did not enter the central nervous system via the olfactory nerve; instead, PrP^d accumulated in elements of the cranial lymphoreticular system prior to neuroinvasion.

The prion diseases, or transmissible spongiform encephalopathies (TSEs), are a group of fatal neurodegenerative diseases that affect animals, including humans. These neurodegenerative diseases are notable for their ability to be transmitted from one animal to another and for their relatively long incubation periods. The natural route(s) of transmission have not been determined. The route of transmission that has been studied experimentally most extensively is the oral pathway. This route is thought to be responsible for the transmission of kuru, bovine spongiform encephalopathy (BSE), transmissible mink encephalopathy (TME), and variant Creutzfeldt-Jakob disease. Experimentally it has been shown that after ingesting food pellets containing infected brain homogenate prions gain access to the central nervous system (CNS) via the autonomic innervation of the gut (7, 27, 34, 36). The prion agent is transported retrogradely to the thoracic spinal cord and the medulla via the sympathetic and parasympathetic nerves, respectively (36). Once the prion agent enters the CNS, there is evidence that spread occurs via synaptically linked neurons (3, 7, 43).

With the exception of BSE-contaminated meat and bone meal thought to be responsible for the outbreak of BSE in the United Kingdom (10) and the cannibalistic practices that spread kuru (18), the source of the prion agent that naturally spreads the TSE among the affected species is not known. Prions have been found in the urine of mice with chronic kidney infections, indicating that urine may be a vector for the spread of prion diseases in some cases (45). Recently, it was reported that infectious prions were found in the saliva and blood of deer with chronic wasting disease, thus indicating that these bodily fluids may be a source of infection in the wild (33). Other potential sources of infectivity that have varying levels of experimental support for their efficacy include placenta (42), decaying carcasses (39), and excreta (39). A recent in vitro study reported that soil can bind prions and maintain infectivity, thus potentially serving as a prion reservoir (25).

Deer, elk, cattle, and sheep are susceptible to the TSE, and each of these species has a well-developed olfactory system that is used for reproductive purposes and to detect predators and food. Thus, it is likely that the nasal cavity of these species would be an initial site of contact with any material that harbors the infectious agent. We tested the hypothesis that the nasal cavity is a site of entry and neuroinvasion for the prion agent by placing a small amount of the hyper (HY) strain of TME agent just inferior to the nostrils of hamsters and observing these animals for the onset of clinical signs. This route was established to be more efficient for causing disease than oral inoculation. Subsequently, we carried out a pathogenesis study to identify the initial site(s) of deposition and subsequent spread of the prion disease-associated isoform of the prion protein (PrP^d). Immunohistochemistry (IHC) was used to identify PrP^d in the nasal cavity, submandibular lymph nodes, cervical lymph nodes, mesenteric lymph nodes, spleen, Peyer's patches, and tongue at 2-week intervals after extranasal (e.n.) exposure to the inoculum.

* Corresponding author. Mailing address: Department of Physical Therapy, Creighton University, 2500 California Plaza, Omaha, NE 68178. Phone: (402) 280-5669. Fax: (402) 280-5692. E-mail: akincaid@creighton.edu.

▽ Published ahead of print on 14 February 2007.

MATERIALS AND METHODS

Animal care. All procedures involving animals were preapproved by the Creighton University Institutional Animal Care and Use Committee and were

TABLE 1. Summary of processed and analyzed tissue sections

Tissue type	Section thickness (μm)	No. of adjacent tissue sections per slide	Sampling interval (μm) of tissue sections:		Avg no. of tissue sections analyzed per infected animal[b]
			Infected animals[a]	Mock-infected animals	
Nasal cavity	5	2–4	200	400	74 (coronal), 34 (sagittal)
NALT[c]	5	2–4	40	100	52 (coronal), 15 (sagittal)
Lymph nodes	7	4–5	56	140	50 (S), 40 (C), 47 (M)
Spleen	7	4	56	140	63
Peyer's patches	7	4	56	140	48
Tongue	7	4	252	504	60

[a] Maximum distance between tissue sections; the sampling frequency was usually higher so the distance between sections was less.
[b] For lymph nodes, the values are subdivided by submandibular (S), cervical (C), and mesenteric (M) lymph nodes.
[c] A subset of sections from the nasal cavity that contain NALT.

done in accordance with the *Guide for the Care and Use of Laboratory Animals* (41). Adult male golden Syrian hamsters were obtained from Harlan Sprague-Dawley (Indianapolis, IN). Hamsters were group housed in standard cages with access to food and water ad libitum.

Animal inoculations. For all inoculations 10 to 50 μl of a 1% (wt/vol) brain homogenate from either an HY TME-infected hamster (containing a $10^{9.3}$ intracerebral [i.c.] 50% lethal dose [LD_{50}]/g) or an uninfected hamster was used. Hamsters receiving e.n. inoculations were anesthetized with ketamine (120 mg/kg) and xylazine (10 mg/kg) intraperitoneally, and 5 μl of inoculum was placed just inferior to each nostril, for a total of 10 μl of inoculum per animal. By not placing the pipette tip inside the nasal cavity the possibility of inadvertent damage to the nasal mucosa with subsequent infection of blood was avoided. The inoculum was observed to be immediately drawn into the nasal cavity after ejection from the pipette. The hamsters were then placed supine until the anesthesia wore off and they began to move, which took between 5 and 10 min. Hamsters inoculated per os were deprived of food for 24 h prior to being given a food pellet that contained 10 μl of inoculum. For i.c. inoculations, hamsters were anesthetized with isoflurane (Webster Veterinary, Kansas City, MO), and 50 μl of inoculum was injected into the right hemisphere by using a 30-gauge needle attached to a 1-ml tuberculin syringe.

Clinical diagnosis and calculation of incubation period. The incubation period was calculated as the length of time in days between exposure to the infectious agent and the onset of clinical signs. Hamsters were observed for the onset and progression of clinical signs three times a week beginning 60 days after inoculation. Clinical signs characteristic of HY TME include an unkempt coat, waddling gait, hyperactive responses to a gentle puff of air or light touch, ataxia, and body tremors.

Efficiency of the nasal route. The endpoint titration of HY TME by the e.n., per os, and i.c. routes was established by inoculating groups of five hamsters with 10-fold serial dilutions of inoculum and determining the incubation period and attack rate. The titer was calculated by using the method of Reed and Muench. The efficiency of the e.n. route was compared to that of the i.c. and per os routes.

IHC. Infected and mock-infected hamsters were anesthetized with isoflurane and perfused transcardially with 50 ml of 0.01 M Dulbecco phosphate buffered saline, followed by 75 ml of McLean's paraformaldehyde-lysine-periodate fixative in preparation for IHC to identify the prion protein. The following tissues were immediately dissected and placed into paraformaldehyde-lysine-periodate for 4 to 5 h at room temperature: nasal cavity, the lymph nodes that drain the nasal cavity (submandibular and deep cervical lymph nodes [40]), the mesenteric lymph nodes, spleen, Peyer's patches from the proximal jejunum, and the tongue. The tissues, except for the nasal cavity, were embedded in paraffin, cut at 7 μm on a rotary microtome, and mounted onto glass slides. The nasal cavity was placed in decalcifying solution at room temperature for 3 to 4 weeks prior to being embedded and cut at 5 μm. Infected and mock-infected tissues for each time point were processed at the same time, using the same reagents. All tissue sections were deparaffinized and subjected to antigen retrieval in formic acid (minimum 95%) for 10 min at room temperature. All of the following steps were carried out at room temperature, and all incubations were separated by two to three rinses with 0.05% Tween in Tris-buffered saline. Endogenous peroxidase and nonspecific antibody binding were blocked by incubating the tissue sections in 0.3% H_2O_2-methanol for 20 min, followed by incubation in 10% normal horse serum for 30 min. Visualization of the prion protein was carried out using the avidin-biotin method. Incubation in mouse anti-prion protein monoclonal antibody (clone 3F4, 1:600; Chemicon, Temecula, CA) was carried out for 2 h at room temperature, followed by incubation in biotinylated horse anti-mouse antibody (1:600; Vector Laboratories, Burlingame, CA) for 30 min. The sections were placed in ABC solution (1:200; Vector Laboratories) for 20 min and then reacted in a solution containing filtered 0.05% diaminobenzidine tetra-

TABLE 2. HY TME inoculation of hamsters by the i.c., per os, and e.n. routes[a]

Brain inoculum dilution[b]	i.c.		Per os		e.n.	
	Incubation period (days)	No. affected/no. inoculated	Incubation period (days)	No. affected/no. inoculated	Incubation period (days)	No. affected/no. inoculated
10^{-1}	ND	ND	158 ± 17	4/5	161 ± 11	5/5
10^{-2}	ND	ND	165 ± 10	2/5	187 ± 39	5/5
10^{-3}	ND	ND	>400	0/5	224 ± 28	4/5[c]
10^{-4}	ND	ND	ND	ND	210	1/5
10^{-5}	ND	ND	ND	ND	>400	0/5
10^{-6}	98 ± 2	5/5	ND	ND	>400	0/5
10^{-7}	134 ± 9	4/5	ND	ND	>400	0/5
10^{-8}	192 ± 54	3/5	ND	ND	>400	0/5
10^{-9}	>400	0/5	ND	ND	>400	0/5
Mock	>400	0/5	>400	0/5	>400	0/5
Titer	$10^{9.3}$		$10^{3.7}$		$10^{5.5}$	

[a] The titers (calculated by the method of Reed and Muench) for the i.c., per os, and e.n. routes are expressed as the LD_{50}/g. Values are expressed as means ± the standard deviation. ND, not done.
[b] Fifty (i.c.) or ten (per os, e.n.) microliters of HY TME brain homogenate was inoculated into each hamster.
[c] Significantly greater attack rate compared to per os inoculation ($P = 0.03$ [Fisher exact test]).

chloride (Sigma, St. Louis, MO) with 0.0015% H_2O_2. This concentration of H_2O_2 was empirically determined to maximize the contrast between immunoreactivity of the normal cellular form of the prion protein, PrP^c, and the abnormal disease-associated form, PrP^d. The sections were counterstained with hematoxylin, dehydrated through graded alcohols, and coverslipped with Cytoseal-XYL (Richard Allan Scientific, Kalamazoo, MI). Control sections were processed identically with either the primary or the secondary antibodies omitted or with a mouse immunoglobulin G isotype control (Abcam, Cambridge, MA) in place of the primary antibody at the same concentration. When additional morphological detail was required, selected adjacent tissue sections were stained with hematoxylin and eosin.

To determine the temporal and spatial spread of PrP^d after exposure to the nasal cavity, tissue sections were examined by using an Olympus BX-40 light microscope and photographed using analySIS software (Soft Imaging System, Lakewood, CO). The sampling frequency and total number of sections of the various tissues that were processed and analyzed are summarized in Table 1. For infected hamsters, regularly spaced tissue sections from the nasal cavity spaced not more than 200 μm apart were inspected for the presence of PrP^d immunoreactivity (PrP^d-ir); for the portion of the nasal cavity that contained the nasal mucosa-associated lymphoid tissue (NALT), the sampling frequency was increased so that the inspected sections were not more than 40 μm apart. For lymph nodes, spleens, and Peyer's patches of infected hamsters, two to four serial sections spaced not more than 56 μm apart were processed and analyzed. The tongue was cut sagittally, and sections from infected hamsters not further apart than 252 μm apart were processed and analyzed. For each tissue the initial time postinoculation of PrP^d deposition was established, as well as the time when all inoculated hamsters demonstrated PrP^d. Sections from each type of tissue were also processed at 22 weeks after inoculation to determine the pattern and extent of PrP^d deposition close to the onset of clinical symptoms.

RESULTS

TME infection after e.n. exposure. The efficiency of the e.n. and per os routes of HY TME infection were determined by calculating the TME titer by endpoint dilution. Based on these data, the LD_{50} values per gram of brain tissue were $10^{5.5}$ for the e.n. route, $10^{3.7}$ for the per os route, and $10^{9.3}$ for the i.c. route. Thus, e.n. exposure was between 10 and 100 times more efficient in transmitting disease than oral inoculation via a food pellet. By comparison, the e.n. route was 1,000 to 10,000 times less efficient in transmitting disease than direct i.c. inoculation (Table 2).

Deposition and accumulation of PrP^d in extraneural structures. IHC was used to identify the initial site and time of deposition and the subsequent temporal spread of PrP^d after e.n. inoculation of HY TME in hamsters that were killed at 2-week intervals after inoculation. The nasal cavity, the submandibular and cervical lymph nodes, the mesenteric lymph nodes, the spleen, Peyer's patches, and the tongue were examined for the presence of PrP^d. The pattern of PrP-ir seen in infected hamsters was compared to that of mock-infected hamsters processed identically (with the same reagents at the same time) for each time point. Discrete, punctate deposits of PrP-ir were seen in selected tissues in infected hamsters but never in mock-infected hamsters and are referred to here as PrP^d (Fig. 1). Omission of either the primary or secondary antibody or replacement of the primary antibody with an isotype control resulted in a complete lack of staining on control sections (data not shown). A summary of the temporal deposition of PrP^d in peripheral tissues is shown in Table 3.

Nasal cavity. Regularly spaced frontal or sagittal tissue sections from the entire extent of the nasal cavity from infected and mock-infected hamsters killed at 2-week intervals after inoculation were examined for the presence of PrP^d. The lining of the nasal cavity included olfactory, respiratory, and follicle-associated epithelia that are attached to a lamina propria (Fig. 2). Immunoreactivity to the 3F4 antibody was restricted to aggregations of lymphoid tissue in the lamina propria of the

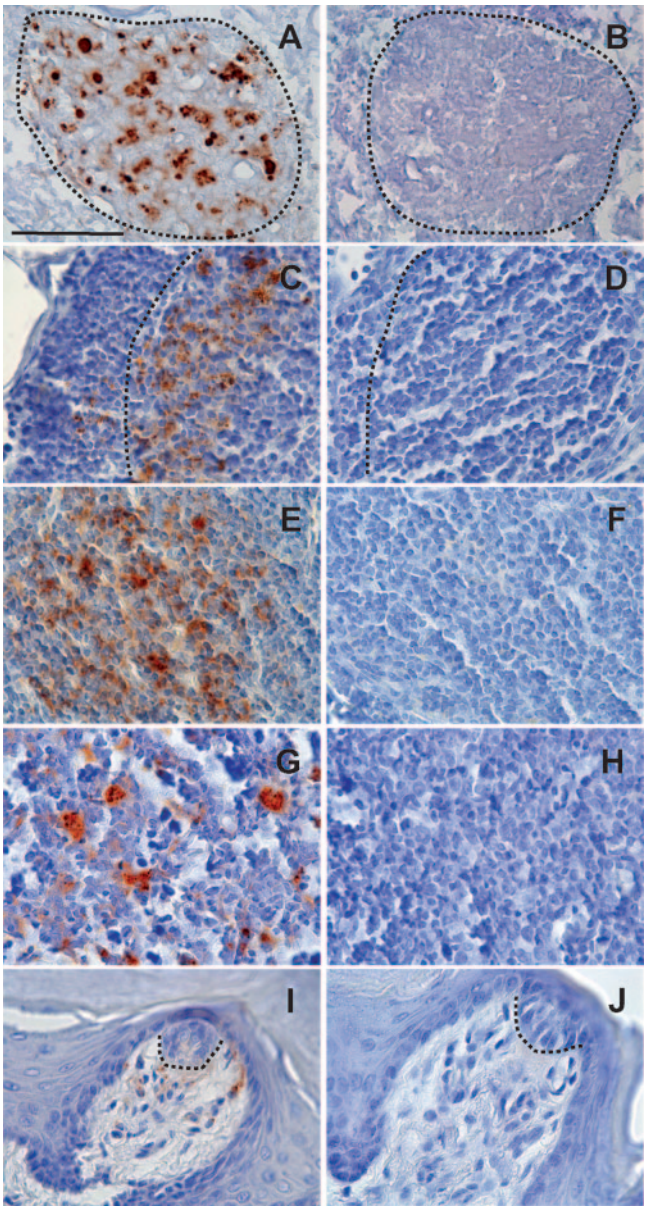

FIG. 1. Deposition of PrP^d in select tissues taken from infected (A, C, E, G, and I) and mock-infected (B, D, F, H, and J) hamsters at 22 weeks after e.n. inoculation. IHC using an antibody to the prion protein was used to identify PrP^d. Matched pairs of tissue sections of the NALT (A and B; NALT outlined by dashed lines), a follicle in the submandibular lymph (C and D; outer edge of follicle outlined by dashed line), white pulp nodule of the spleen (E and F), Peyer's patch (G and H), and a fungiform papillae of the tongue (I and J; base of taste bud outlined by dashed line) from infected and mock-infected hamsters that were processed identically. Note the punctate deposits of PrP^d that were seen only in tissues of hamsters that were inoculated e.n. with HY TME and the lack of PrP^d in the same tissues taken from the e.n. mock-infected hamsters. Bar, 50 μm.

TABLE 3. Temporal deposition of PrP^d in extraneural structures after e.n. inoculation

Structure	No. of PrP^d-positive hamsters/total no. of e.n.-inoculated hamsters at time point (in wk) postinoculation:										
	2	4	6	8	10	12	14	16	18	20	22
Nasal cavity: NALT	0/3	3/3	3/3	3/3	3/3	3/3	3/3	3/3	ND	ND	3/3
Submandibular lymph node	0/3	1/3	2/3	3/3	3/3	3/3	3/3	3/3	ND	ND	3/3
Cervical lymph node	ND	ND	0/3	1/3	3/3	2/2	3/3	3/3	ND	ND	3/3
Mesenteric lymph node	ND	ND	ND	ND	ND	0/3	2/3	1/3	1/3	3/3	3/3
Spleen	ND	ND	ND	ND	0/3	0/3	2/3	3/3	ND	ND	3/3
Peyer's patch	ND	ND	ND	ND	ND	0/3	1/3	1/3	2/3	3/3	3/3
Tongue	ND	ND	ND	ND	ND	ND	ND	ND	0/3	1/3	2/3

floor of the nasal cavity at the entrance of the nasopharyngeal duct (Fig. 2D). This unencapsulated lymphoid tissue was organized into follicles and has been designated by others as NALT (31, 47, 51). There was no immunoreactivity in the olfactory epithelium (Fig. 2B), the respiratory epithelium (Fig. 2C), or the vomeronasal organ (data not shown) in any hamster, at any time point after inoculation. The only site of discrete, punctate staining in the nasal cavity of infected hamsters was in the NALT (Fig. 1A, 2D, and 3). Punctate, discrete immunoreactivity was never seen in the NALT or in any of the tissues examined from any of the mock-infected hamsters (Fig. 1B, 1D, 1F, 1H, and 1J).

There was no staining in the nasal cavity of infected hamsters 2 weeks after inoculation. Beginning at 4 weeks after inoculation a few discrete, granular depositions of PrP^d of various size were visible in the NALT of all three infected hamsters bilaterally (Table 3 and Fig. 3A). The immunoreactive accumulations were as large as 2 to 3 μm in diameter and appeared to be primarily located in the cytoplasm or on the surface of relatively large, pale staining cells located between lymphocytes (Fig. 3). We did not identify these cells using any cell-specific markers but, based on their size, location, and previous reports, the PrP^d appeared to be associated with macrophages and follicular dendritic cells (1, 2, 28, 35, 46, 52). At every subsequent time point all three of the infected hamsters had PrP^d in the NALT, and the amount of PrP^d gradually increased in hamsters at later time points postinfection (Fig. 3). In hamsters that survived 22 weeks after inoculation, the PrP^d was located through the entire rostral-caudal and medial-lateral extent of the NALT (Fig. 3D).

Lymph nodes. PrP^d was first noted in the follicles of submandibular lymph nodes of one of the three infected hamsters 4 weeks after inoculation. It was present in two of three infected hamsters 6 weeks after inoculation and in all three infected hamsters at all subsequent time points (Table 3). The amount and pattern of deposition of PrP^d was variable from one hamster to the next within a group, but a gradual increase in PrP^d immunoreactivity over time was consistently observed (Fig. 4A). Uninfected lymph nodes were present among the infected lymph nodes, even at later time points, and infected follicles within a given lymph node were sometimes, but not always, adjacent to one another (Fig. 4A). Initially, PrP^d was only noted in one follicle, but at later time points the maximum number of PrP^d-ir follicles in a single lymph node increased to as many as 11. Just as in the NALT, PrP^d was always located between lymphocytes and appeared to be associated with follicular dendritic cells and macrophages (1, 2, 28, 35, 46, 52). PrP^d was first noted in the cervical lymph nodes of one of the three infected hamsters 8 weeks after inoculation and was present in all three infected hamsters at all subsequent time points (Table 3). The deposition of PrP^d within the cervical lymph nodes was similar in appearance to that seen in submandibular lymph nodes, but the amount of immunoreactivity was consistently less (Fig. 4C), and PrP^d did not accumulate in multiple follicles over time. The maximum number of PrP^d-ir follicles seen in a cervical lymph node was six, which was seen in a hamster at the earliest time point at which a cervical lymph node was determined to be immunopositive. PrP^d was first noted in the mesenteric lymph nodes of two infected hamsters at 14 weeks after inoculation but was not seen in all three infected hamsters till 20 weeks after inoculation (Table 3). The number of PrP^d-ir follicles and the amount immunoreactivity per immunopositive follicle was much less than what was noted in either the cervical or the submandibular lymph nodes (Fig. 4E), but the location of PrP^d was the same between lymphocytes and in association with presumptive macrophages and follicular dendritic cells.

Spleen and Peyer's patches. PrP^d was first noted in white pulp nodules of the spleen in two of three hamsters 14 weeks after inoculation with HY TME (Table 3; Fig. 5A). It was present in all three hamsters at 16 and 22 weeks after inoculation. Although the number of immunopositive nodules increased with time from inoculation, the maximum number of PrP^d-ir nodules on any section of spleen was five, which represented less than half the number of nodules present. The pattern of immunoreactivity was similar to what has been reported previously in mice inoculated i.c. (24), with staining predominantly in the germinal center of white pulp nodules and less-frequent staining in the peripheral white pulp. Although no additional markers were used to identify specific cell types, the staining was clearly restricted to nonlymphocytes (Fig. 5B). In Peyer's patches PrP^d was first noted in one hamster 14 weeks after inoculation and in one hamster at 16 weeks (Table 3). At 18 weeks, PrP^d was seen in the Peyer's patches of two of the three infected hamsters and in all three infected hamsters at 20 and 22 weeks after inoculation (Fig. 5C). The deposition of PrP^d in Peyer's patches was similar to what has been reported previously for orally inoculated hamsters (6). PrP^d was located between lymphocytes and in, or on, large cells, presumably macrophages and/or follicular dendritic cells (Fig. 1G and 5D). Although the majority of PrP^d was located within the Pey-

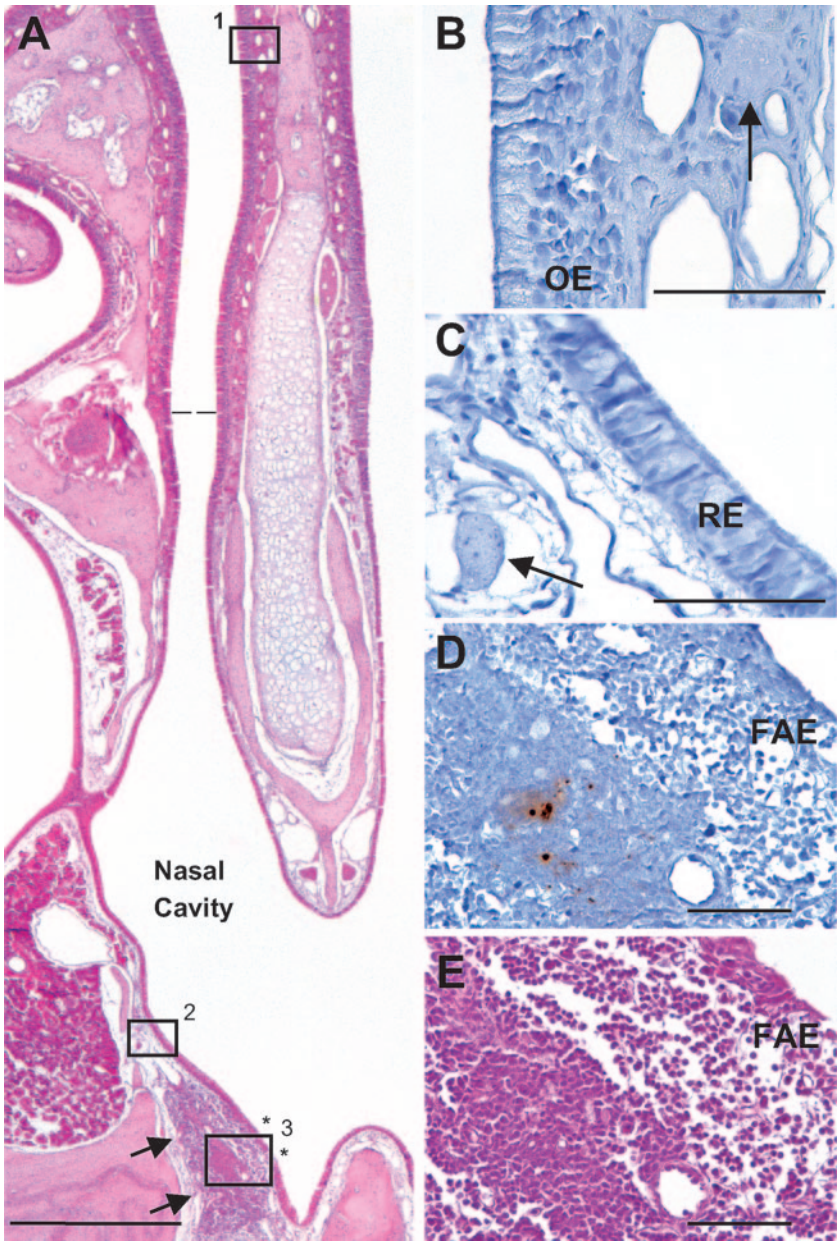

FIG. 2. Hamster nasal cavity with the different types of covering epithelia and the NALT in the lamina propria in the floor of the nasal cavity. (A) A low-power view of a hematoxylin-and-eosin-stained coronal section of half of the nasal cavity from a hamster shows the midline nasal septum, the position of the NALT (indicated by arrows), the boundary between the olfactory and respiratory epithelia (dotted line), and the extent of the follicle-associated epithelium overlying the NALT (asterisks). The olfactory epithelium lines the nasal cavity above the dotted line, while respiratory epithelium lines most of the nasal cavity below the dotted line. The follicle-associated epithelium lines a small part of the nasal cavity that overlies the NALT. Adjacent tissue sections from the areas indicated by boxes 1 to 3 in panel A from a hamster 6 weeks after e.n. inoculation were processed for PrP^d using IHC and shown at higher magnifications in panels B to D, respectively. Note the lack of PrP^d in the olfactory epithelium (B) and the respiratory epithelium (C) and the adjacent nerve fascicles in the lamina propria (arrows). (D) Punctate deposits of PrP^d were identified only in the NALT of hamsters inoculated with HY TME e.n. and not in any other structures. (E) Hematoxylin and eosin staining of hamster NALT, view enlarged from the tissue section in panel A, reveals the morphology of the hamster NALT, which is made up largely of lymphoid tissue. OE, olfactory epithelium; RE, respiratory epithelium; FAE, follicle-associated epithelium. Bars: A, 500 μm; B, C, D, and E, 50 μm.

er's patches, there was also intense staining in neurons of nearby submucosal plexi in hamsters that had multiple Peyer's patches labeled (not shown) and in the lamina propria of the villi of several hamsters (not shown).

Tongue. PrP^d was first noted in the tongues of one of three hamsters at 20 weeks postinfection and two of three hamsters at 22 weeks postinfection. The staining was seen in a small percentage (<10%) of fungiform papillae, often at the

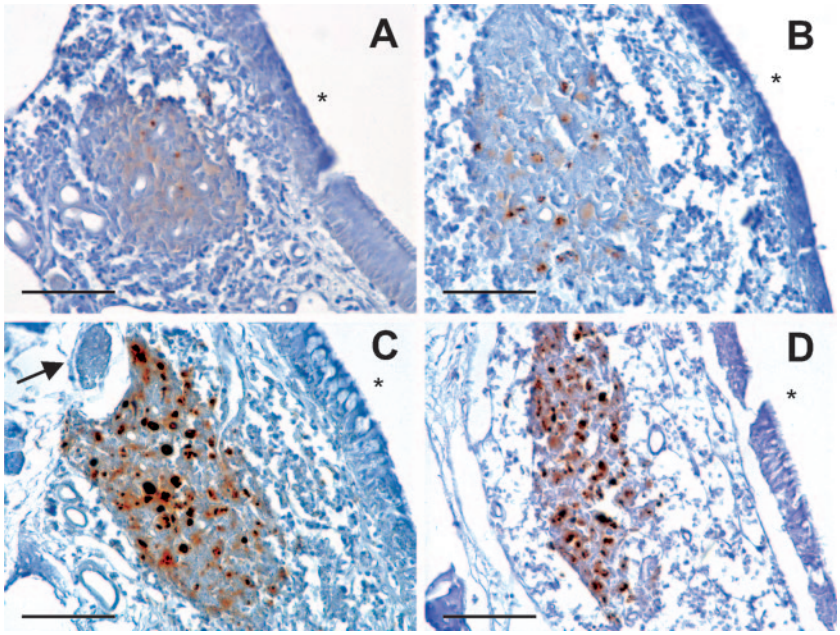

FIG. 3. Progressive accumulation of PrP^d in the NALT of hamsters inoculated with HY TME. (A to D) Tissue sections that include depositions of PrP^d in the NALT from hamsters at 4 weeks (A), 10 weeks (B), 16 weeks (C), and 22 weeks (D) after e.n. inoculation. Note the increased amount of PrP^d immunoreactivity in the NALT at the various times postinfection. There is an increase in both the number of punctate deposits and the size of the deposits. The asterisk indicates the air space of the nasal cavity in each picture, and the arrow indicates a nerve fascicle (C). Bars, 50 μm.

base of taste buds, but also in the lamina propria and in a small number of nerve fascicles on the dorsum or tip of the tongue (Fig. 1I and J). PrP^d was not seen in skeletal muscle cells or in the stratified squamous epithelium of either the dorsal or ventral surfaces of the tongue in any hamster.

DISCUSSION

Other than a brief mention of mice being infected intranasally with scrapie agent in a 1963 publication (13), this is the first report of prion infection after exposure of the agent to the nasal cavity. All hamsters e.n. infected with a high dose of HY TME brain homogenate became clinically ill with an incubation period similar to that of hamsters infected per os with the same dose of HY TME agent. Of particular interest was the finding that the nasal route was more efficient than the oral route, based on the calculated LD_{50} per gram of tissue (Table 2). Thus, a smaller dose of agent introduced to a hamster via the nasal cavity was more likely to result in disease than if a food pellet containing the inoculum was ingested. However, we cannot exclude the possibility that other modes of oral infection (e.g., direct application to oral mucosa) may change the relative differences between these two routes of infection. This route of infection may be of significance to the natural transmission of disease, since animals that naturally develop the TSE are olfactory driven and use their olfactory sense for a variety of basic life activities such as securing food, detecting predators, and reproduction. Therefore, they may expose their nasal cavity to the infectious agent as they use their sense of smell to explore their environment. The placement of the agent just outside of the nasal cavity in the present study was intentional so as to avoid any unintentional damage to the epithelia that line the nasal cavity with the pipette tip, since there are nerves and blood vessels located in the underlying lamina propria that could unintentionally serve as a site of entry for the agent.

PrP^d was identified using IHC in the NALT of the nasal cavity of all infected hamsters between 4 and 22 weeks postinfection, but not in the olfactory epithelium and nerve fascicles, as we had hypothesized. There were several reasons to expect that the olfactory nerve might serve as a route of entry for prion infection after nasal cavity exposure, including the expression of PrP^c by olfactory receptor neurons (17), which is necessary for prion replication (8); the ability of olfactory receptor neurons to support prion replication (11, 54); and the involvement of olfactory structures in chronic wasting disease of deer and elk (48, 53). However, in the experiments reported here none of the cells of the olfactory epithelium, 75 to 85% of which are olfactory receptor neurons (14), and no associated nerve fascicles, which include the axons of these neurons, accumulated any detectable amount of PrP^d at any point after exposure to the agent. Thus, the olfactory neurons were not responsible for transporting prions into the CNS of these animals. Instead, it appears that the neuroinvasion of this strain of prion in this animal model is another example where the agent initially accumulates in peripheral lymphoid tissue and is subsequently transported to the CNS (recently reviewed in reference 32).

The detection of PrP^d in the NALT of all infected hamsters at 4 weeks after inoculation, which represents 14% of the incubation period, is much earlier than the first detection of agent in the Peyer's patches in the present study (14 weeks; 50% of the incubation period). This interval is also

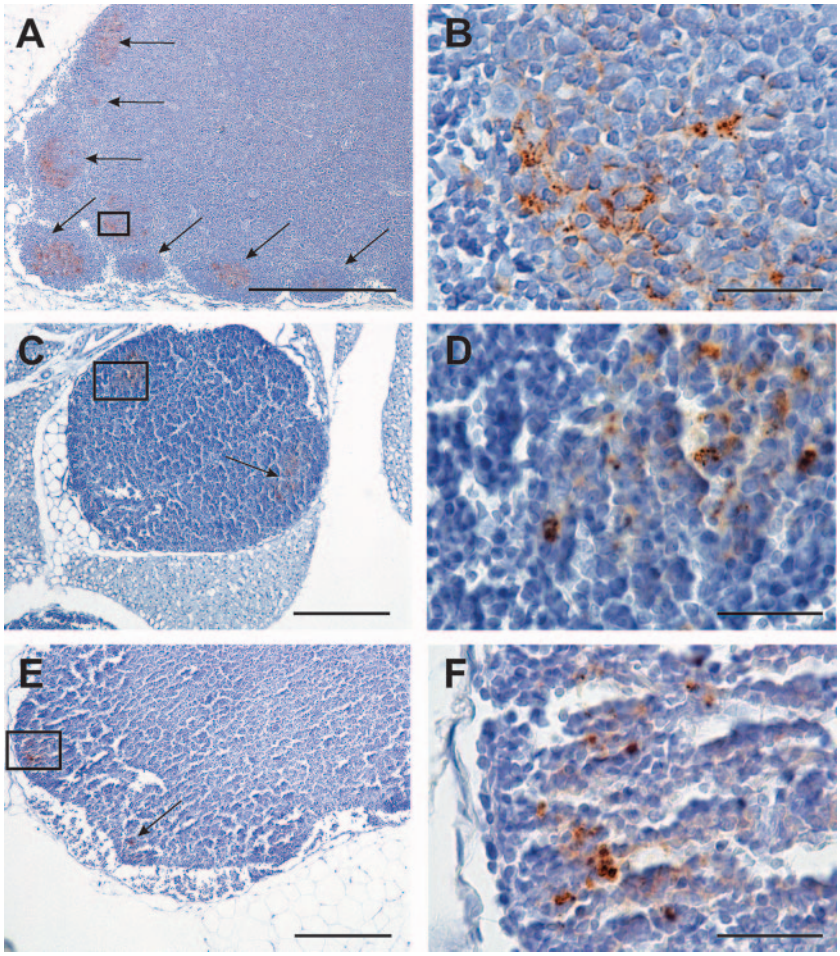

FIG. 4. PrP^d in lymph nodes after e.n. inoculation. (A) Low-power view of PrP^d in multiple follicles (indicated by arrows) of a submandibular lymph node of a hamster 14 weeks after e.n. inoculation. (B) High-power view of the area outlined by the box in panel A. The PrP^d is located in, or on, cells and cell processes between the lymphocytes of the submandibular lymph node. (C) Low-power view of a cervical lymph node of a hamster at 22 weeks postinoculation. Note the PrP^d is found in only two follicles (box and arrow). (D) High-power view of PrP^d in the area outlined by the box in panel C. PrP^d is located between the lymphocytes of the follicle. (E) Low-power view of a mesenteric lymph node of a hamster at 22 weeks postinoculation. Note that the PrP^d is limited to two follicles (box and arrow). (F) High-power view of PrP^d in the area outlined by the box in panel E. Note the punctate staining located between the lymphocytes of the follicle. Bars: A, 500 μm; C and E, 200 μm; B, D, and F, 50 μm.

earlier than other reports of peripheral accumulation of the agent in lymphoid tissue after per os inoculation of a similar prion strain in hamsters (6). Whether this relatively early and progressive accumulation of agent in lymphatic tissue after a nontraumatic inoculation is responsible for the greater efficiency of this route compared to the per os route in this model of prion infection, or is just coincident, remains to be determined.

The NALT in rodents are a component of the mucosa-associated lymphoid tissue that includes bronchus-associated lymphoid tissue and Peyer's patches (31, 47). The NALT are paired, unencapsulated lymphoid structures located in the floor of the nasal cavity near the entrance to the pharynx that are thought to be analogous to the tonsils and adenoids in humans (29, 31). Rodent NALT is covered by a follicle-associated epithelium that includes microfold cells (M cells) and consists of follicles containing T cells, B cells, macrophages, and follicular dendritic cells (19, 22, 30).

The temporal pattern of PrP^d accumulation after e.n. exposure is consistent with initial accumulation in the NALT, followed quickly by spread to the draining submandibular lymph nodes and then to the regional deep cervical lymph nodes. From there the agent could enter the lymph and blood and spread to distant lymph nodes and the spleen, since detection of PrP^d in these structures occurred 6 weeks later at 14 weeks after inoculation. Alternatively, the agent may gain access to the lymph nodes and blood via unknown non-NALT routes.

PrP^d was detected in the Peyer's patches of one of three infected hamsters at 14 and 16 weeks after inoculation. These time points represent 50 and 57% of the incubation period. Given that neuroinvasion of the spinal cord and brain usually occurs between 25 and 50% of the incubation period after non-neural inoculation (26), the presence of PrP^d in the Peyer's patches at these and subsequent time points in the incubation period of this route of infection suggests the spread of the agent from the CNS to these structures, as opposed to

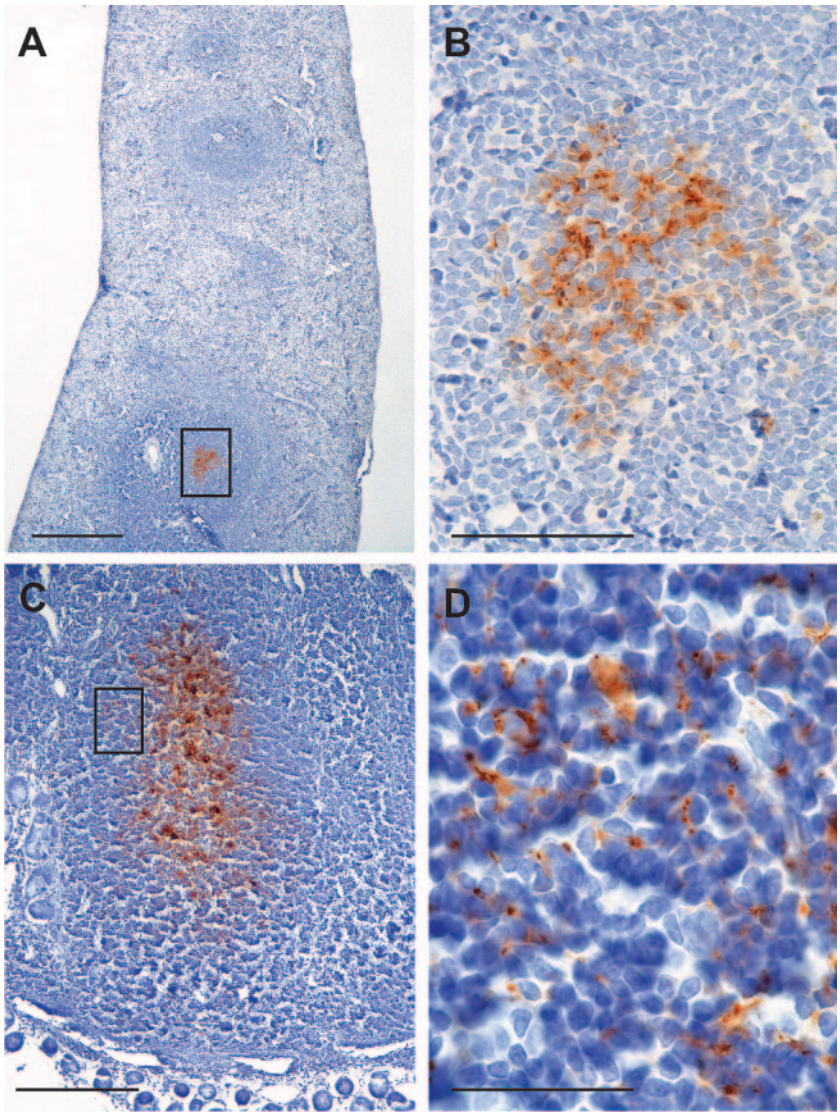

FIG. 5. PrP^d in the spleen and Peyer's patches after e.n. inoculation. (A) PrP^d is restricted to a single lymphoid follicle in the white pulp of the spleen of a hamster 14 weeks after e.n. inoculation. (B) High-power view of the area outlined in the box in panel A. PrP^d is in, or on, cells and cell processes located between the lymphocytes. (C) PrP^d in a Peyer's patch from a hamster 20 weeks after e.n. inoculation. (D) High-power view of the area outlined in the box in panel C. PrP^d is in, or on, cells and cell processes located between the lymphocytes. Bars: A, 200 μm; B, 50 μm; C, 100 μm; D, 25 μm.

being an entry point for neuroinvasion. Alternatively, some of the infectious agent may have been swallowed after passing through the nasopharynx and reached the gut to accumulate in the Peyer's patches at these later time points. The relatively late appearance of PrP^d in the tongue (>70% of the incubation period) indicates that the agent did not enter the CNS via the nerves that innervate this structure but were transported centrifugally from the infected brainstem to the tongue, as has been reported previously (11).

Whether neuroinvasion in this model of prion infection occurs via direct innervation of the NALT (30, 47) (Fig. 3C), the sympathetic fibers that innervate lymph nodes and spleen (15, 16, 20, 21), the well-documented innervation of the Peyer's patches (6, 34), or some combination of these structures remains to be determined. Other potential routes of entry from the nasal cavity to the CNS include the trigeminal and parasympathetic innervation of nasal cavity structures (14).

Although there has not been a documented case of natural transmission via the nasal cavity to date, sheep, deer, and elk possess lymphoid tissue in their nasopharynx (referred to as either NALT or pharyngeal tonsils), and these species transmit the TSE agent horizontally between animals within a herd (9, 12, 23, 37, 38, 49). Support for the nasal cavity as a potential natural route of entry includes the finding that lymphoid follicles in the nasal septum of free-ranging and captive mule deer that were dying of chronic wasting disease contained the proteinase-resistant isoform of the prion protein (48) and the recent report that NALT can support prion accumulation after i.c. inoculation (11).

Thus, in addition to neuroinvasion after experimental exposure to abraded tongue (4) and skin (50), to intact gut epithelium (5, 7, 27), and to conjunctiva (44), prions may efficiently enter the CNS and cause disease following exposure to the intact nasal cavity.

ACKNOWLEDGMENTS

This study was supported by the National Center for Research Resources (P20-RR0115635-6) and by revenue from the Nebraska Tobacco Settlement awarded to Creighton University by the State of Nebraska.

The content of this study is solely the responsibility of the authors and does not necessarily represent the official views of the State of Nebraska.

We thank Rachel Rhatigan, Maria Christensen, and Meghan Sheehan for excellent technical assistance with this rather long project.

REFERENCES

1. **Andreoletti, O., P. Berthon, E. Levavasseur, D. Marc, F. Lantier, E. Monks, J.-M. Elsen, and F. Schelcher.** 2002. Phenotyping of protein-prion (PrPsc)-accumulating cells in lymphoid and neural tissues of naturally scrapie-affected sheep by double-labeling immunohistochemistry. J. Histochem. Cytochem. **50:**1357–1370.
2. **Andreoletti, O., P. Berthon, D. Marc, P. Sarradin, J. Grosclaude, L. van Keulen, F. Schelcher, J.-M. Elsen, and F. Lantier.** 2000. Early accumulation of PrP^{sc} in gut-associated lymphoid and nervous tissues of susceptible sheep from a Romanov flock with natural scrapie. J. Gen. Virol. **81:**3115–3126.
3. **Bartz, J. C., A. E. Kincaid, and R. A. Bessen.** 2002. Retrograde transport of transmissible mink encephalopathy within descending motor tracts. J. Virol. **76:**5759–5768.
4. **Bartz, J. C., A. E. Kincaid, and R. A. Bessen.** 2003. Rapid prion neuroinvasion following tongue infection. J. Virol. **77:**583–591.
5. **Beekes, M., E. Baladuf, and H. Diringer.** 1996. Sequential appearance and accumulation of pathognomonic markers in the central nervous system of hamsters orally infected with scrapie. J. Gen. Virol. **77:**1925–1934.
6. **Beekes, M., and P. A. McBride.** 2000. Early accumulation of pathological PrP in the enteric nervous system and gut-associated lymphoid tissue of hamsters orally infected with scrapie. Neurosci. Lett. **278:**181–184.
7. **Beekes, M., P. A. McBride, and E. Baladuf.** 1998. Cerebral targeting indicates vagal spread of infection in hamster fed orally with scrapie. J. Gen. Virol. **79:**601–607.
8. **Blattler, T., S. Brandner, A. J. Raeber, M. A. Klein, T. Voigtlander, C. Weissmann, and A. Aguzzi.** 1997. PrP-expressing tissue required for transfer of scrapie infectivity from spleen to brain. Nature **389:**69–73.
9. **Chen, W., M. R. Alley, and B. W. Manktelow.** 1989. Respiratory tract-associated lymphoid tissue in conventionally raised sheep. J. Comp. Pathol. **101:**327–340.
10. **Collee, J. G., and R. Bradley.** 1997. BSE: a decade on-part 1. Lancet **349:** 636–642.
11. **DeJoia, C., B. Moreaux, K. O. O'Connell, and R. A. Bessen.** 2006. Prion infection of oral and nasal mucosa. J. Virol. **80:**4546–4556.
12. **Dyce, K. M., W. O. Sack, and C. J. G. Wensing.** 1996. The head and ventral neck of ruminants, p. 631–652. *In* Textbook of veterinary anatomy, 2nd ed. The W. B. Saunders Co., Philadelphia, PA.
13. **Eklund, C. M., W. J. Hadlow, and R. C. Kennedy.** 1963. Some properties of the scrapie agent and its behavior in mice. Proc. Soc. Exp. Biol. Med. **112:**974–979.
14. **Farbman, A. I.** 1992. Structure of olfactory mucous membrane, p. 24–74. *In* Cell biology of olfaction. Cambridge University Press, Cambridge, England.
15. **Felten, D. L., K. D. Ackerman, S. J. Wiegand, and S. Y. Felten.** 1987. Noradrenergic sympathetic innervation of the spleen: 1. Nerve fibers associate with lymphocytes and macrophages in specific compartments of the splenic white pulp. J. Neurosci. Res. **18:**28–36.
16. **Felten, D. L., S. Livnant, S. Y. Felten, S. L. Carlson, D. L. Bellinger, and P. Yeh.** 1984. Sympathetic innervation of lymph nodes in mice. Brain Res. Bull. **13:**693–699.
17. **Ford, M. J., L. J. Burton, R. J. Morris, and S. M. Hall.** 2002. Selective expression of prion protein in peripheral tissues of the adult mouse. Neuroscience **113:**177–192.
18. **Gajdusek, D. C.** 1997. Unconventional viruses and the origin and disappearance of kuru. Science **197:**943–960.
19. **Giannasca, P. J., J. A. Boden, and T. P. Monath.** 1997. Targeted delivery of antigen to hamster nasal lymphoid tissue with M-cell directed lectins. Infect. Immun. **65:**4288–4298.
20. **Glatzel, M., F. L. Heppner, K. M. Albers, and A. Aguzzi.** 2001. Sympathetic innervation of lymphoid organs is rate limiting for prion neuroinvasion. Neuron **31:**25–34.
21. **Heggebo, R., L. Gonzalez, C. M. Press, G. Gunnes, A. Espenes, and M. Jeffrey.** 2003. Disease-associated PrP in the enteric nervous system of scrapie-affected Suffolk sheep. J. Gen. Virol. **84:**1327–1338.
22. **Heritage, P. L., B. J. Underdown, A. L. Arsenault, D. P. Snider, and M. R. McDermott.** 1997. Comparison of murine nasal-associated lymphoid tissue and Peyer's patches. Am. J. Respir. Crit. Care Med. **156:**1256–1262.
23. **Hunter, N.** 2003. Scrapie and experimental BSE in sheep. Br. Med. Bull. **66:**171–183.
24. **Jeffrey, M., G. McGovern, C. M. Goodsir, K. L. Brown, and M. E. Bruce.** 2000. Sites of prion protein accumulation in scrapie-infected mouse spleen revealed by immuno-electron microscopy. J. Pathol. **191:**323–332.
25. **Johnson, C. J., K. E. Phillips, P. T. Schramm, D. McKenzie, J. M. Aiken, and J. A. Pedersen.** 2006. Prions adhere to soil minerals and remain infectious. PLoS Pathog. **2:**296–302.
26. **Kimberlin, R. H., and C. A. Walker.** 1979. Pathogenesis of mouse scrapie: dynamics of agent replication in spleen, spinal cord and brain after infection by different routes. J. Comp. Pathol. **89:**551–562.
27. **Kimberlin, R. H., and C. A. Walker.** 1989. Pathogenesis of scrapie in mice after intragastric infection. Virus. Res. **12:**213–220.
28. **Kitamoto, T., T. Muramoto, S. Mohri, K. Doh-Ura, and J. Tateishi.** 1991. Abnormal isoform of prion protein accumulates in follicular dendritic cells in mice with Creutzfeldt-Jakob disease. J. Virol. **65:**6292–6295.
29. **Kraal, G.** 2005. Nasal-associated lymphoid tissue, p. 415–422. *In* J. Mestecky, M. E. Lamm, W. Strober, J. Bienenstock, J. R. McGhee, and L. Mayer (ed.), Mucosal immunology, 3rd ed., vol. 1. Elsevier Academic Press, London, England.
30. **Kuper, C. F., D. M. H. Hameleers, J. P. Bruijntjes, I. van der Ven, J. Biewenga, and T. Sminia.** 1990. Lymphoid and non-lymphoid cells in nasal-associated lymphoid tissue (NALT) in the rat. Cell Tissue Res. **259:**371–377.
31. **Kuper, C. F., P. J. Koornstra, D. M. H. Hameleers, J. Biewenga, B. J. Spit, A. M. Duijvestijn, P. J. C. van Breda Vriesman, and T. Sminia.** 1992. The role of nasopharyngeal lymphoid tissue. Immunol. Today **13:**219–224.
32. **Mabbott, N. A., and G. G. MacPherson.** 2006. Prions and their lethal journey to the brain. Nat. Rev. Microbiol. **4:**201–211.
33. **Mathiason, C. K., J. G. Powers, S. J. Dahmes, D. A. Osborn, K. V. Miller, R. J. Warren, G. L. Mason, S. A. Hays, J. Hayes-Klug, D. M. Seelig, M. A. Wild, L. L. Wolfe, T. R. Spraker, M. W. Miller, C. J. Sigurdson, G. C. Telling, and E. A. Hoover.** 2006. Infectious prions in the saliva and blood of deer with chronic wasting disease. Science **314:**133–136.
34. **McBride, P. A., and M. Beekes.** 1999. Pathological PrP is abundant in sympathetic and sensory ganglia of hamsters fed with scrapie. Neurosci. Lett. **265:**135–138.
35. **McBride, P. A., P. Eikelenboom, G. Kraal, H. Fraser, and M. E. Bruce.** 1992. PrP protein is associated with follicular dendritic cells of spleens and lymph nodes in uninfected and scrapie-infected mice. J. Pathol. **168:**413–418.
36. **McBride, P. A., W. J. Schulz-Schaeffer, M. Donaldson, M. Bruce, H. Diringer, H. A. Kretzschmar, and M. Beekes.** 2001. Early spread of scrapie from the gastrointestinal tract to the central nervous system involves autonomic fibers of the splanchnic and vagus nerves. J. Virol. **75:**9320–9327.
37. **Miller, M. W., and M. A. Wild.** 2004. Epidemiology of chronic wasting disease in captive white-tailed deer and mule deer. J. Wild. Dis. **40:**320–327.
38. **Miller, M. W., and E. S. Williams.** 2003. Horizontal prion transmission in mule deer. Nature **425:**35–36.
39. **Miller, M. W., E. S. Williams, N. T. Hobbs, and L. L. Wolfe.** 2004. Environmental sources of prion transmission in mule deer. Emerg. Infect. Dis. **10:**1003–1006.
40. **Miotti, V.** 1961. Die lymphknoten und lymphgefasse des syrischen goldhamsters. Acta Anat. **46:**192–216.
41. **National Research Council.** 1996. Guide for the care and use of laboratory animals. National Academy Press, Washington, DC.
42. **Race, R., A. Jenny, and D. Sutton.** 1998. Scrapie infectivity and proteinase K-resistant prion protein in sheep placenta, brain, spleen, and lymph node: implication for transmission and antemortem diagnosis. J. Infect. Dis. **178:** 949–953.
43. **Scott, J. R., D. Davies, and H. Fraser.** 1992. Scrapie in the central nervous system: neuroanatomical spread of infection and Sinc control of pathogenesis. J. Gen. Virol. **73:**1637–1644.
44. **Scott, J. R., J. D. Foster, and H. Fraser.** 1993. Conjunctival instillation of scrapie in mice can produce disease. Vet. Microbiol. **34:**305–309.
45. **Seeger, H., M. Heikenwalder, N. Zeller, J. Kranich, P. Schwarz, A. Gaspert, B. Seifert, G. Miele, and A. Aguzzi.** 2005. Coincident scrapie infection and nephritis lead to urinary prion excretion. Science **310:**324–326.
46. **Sigurdson, C. J., C. Barillas-Mury, M. W. Miller, B. Oesch, L. J. M. van Keulen, J. P. M. Langeveld, and E. A. Hoover.** 2002. PrP^{CWD} lymphoid cell targets in early and advanced chronic wasting disease of mule deer. J. Gen. Virol. **83:**2617–2628.
47. **Spit, B. J., E. G. J. Hendriksen, J. P. Bruijntes, and C. F. Kuper.** 1989. Nasal lymphoid tissue in the rat. Cell Tissue Res. **255:**193–198.
48. **Spraker, T. R., R. R. Zink, B. A. Cummings, M. A. Wild, M. W. Miller, and K. I. O'Rourke.** 2002. Comparison of histological lesions and immunohistochemical staining of proteinase-resistant prion protein in a naturally occurring spongiform encephalopathy of free-ranging mule deer (*Odocoileus*

hemionus) with those of chronic wasting disease of captive mule deer. Vet. Pathol. **39:**110–119.
49. **Stanley, A. C., J. F. Huntley, M. Jeffrey, and D. Buxton.** 2001. Characterization of ovine nasal-associated lymphoid tissue and identification of M cells in the overlying follicle-associated epithelium. J. Comp. Pathol. **125:**262–270.
50. **Taylor, D. M., I. McConnell, and H. Fraser.** 1996. Scrapie infection can be established readily through skin scarification in immunocompetent but not immunodeficient mice. J. Gen. Virol. **77:**1595–1599.
51. **Uraih, L. C., and R. R. Maronpot.** 1990. Normal histology of the nasal cavity and application of special techniques. Environ. Health Perspect. **85:**187–208.
52. **Van Keulen, L. J. M., B. E. C. Schreuder, R. H. Meloen, G. Mooij-Harkes, M. E. W. Vromans, and J. P. M. Langeveld.** 1996. Immunohistochemical detection of prion protein in lymphoid tissues of sheep with natural scrapie. J. Clin. Microbiol. **34:**1228–1231.
53. **Williams, E. S., and S. Young.** 1993. Neuropathology of chronic wasting disease of mule deer (*Odocoileus hemionus*) and elk (*Cervus elaphus nelsoni*). Vet. Pathol. **30:**36–45.
54. **Zanusso, G., S. Ferrari, F. Cardone, P. Zampieri, M. Gelati, M. Fiorini, A. Farinazzo, M. Gardiman, T. Cavallaro, M. Bentivoglio, P. G. Righetti, M. Pocchiari, N. Rizzuto, and S. Monaco.** 2003. Detection of pathologic prion protein in the olfactory epithelium in sporadic Creutzfeldt-Jakob disease. N. Engl. J. Med. **348:**711–719.